Mechanical stress regulates insulin sensitivity through integrin-dependent control of insulin receptor localization

Jung Kim[1, 2], David Bilder[2]* and Thomas P. Neufeld[1]*

SUPPLEMENTAL MATERIAL

Supplemental Figures S1 to S6

Legends to Supplemental Movies S1 & S2

Supplemental Table S1

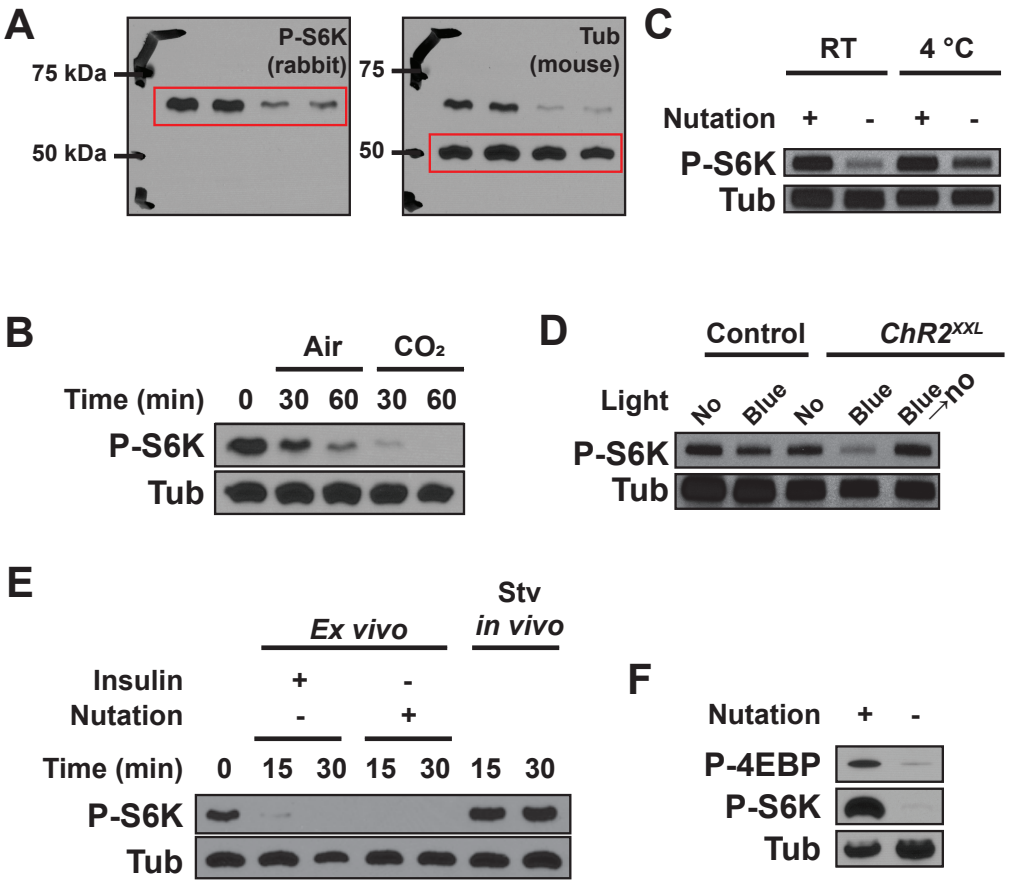

Supplemental Figure S1

(A) Original scans of blots shown in Fig. 1B.

(B) Timecourse of fb-TOR activity in response to starvation alone or starvation with CO_2 anesthesia. Inhibition of larval body movement by CO_2 anesthesia during starvation resulted in a more rapid loss of fb-TOR activity compared to starvation of motile larvae.

(C) Fb-TOR activity requires nutation both at room temperature (RT) and 4 °C during *ex vivo* incubation of larval carcasses.

(D) *Ok6-Gal4* (Control) and *Ok6-Gal4>UAS-ChR2-XXL* larvae were cultured for 15 minutes under blue light (Blue) to inhibit larval movement or no-light control (No). Optogenetic paralysis caused a loss of fb-TOR activity, which was restored by removal of the blue light for an additional 15 min.

(E) Fb-TOR activity was lost within 15 min of incubation *ex vivo* in the absence of nutation or insulin.

(F) The levels of phosphorylated 4EBP and S6K showed a similar requirement for nutation during *ex vivo* incubation in M3 media + insulin.

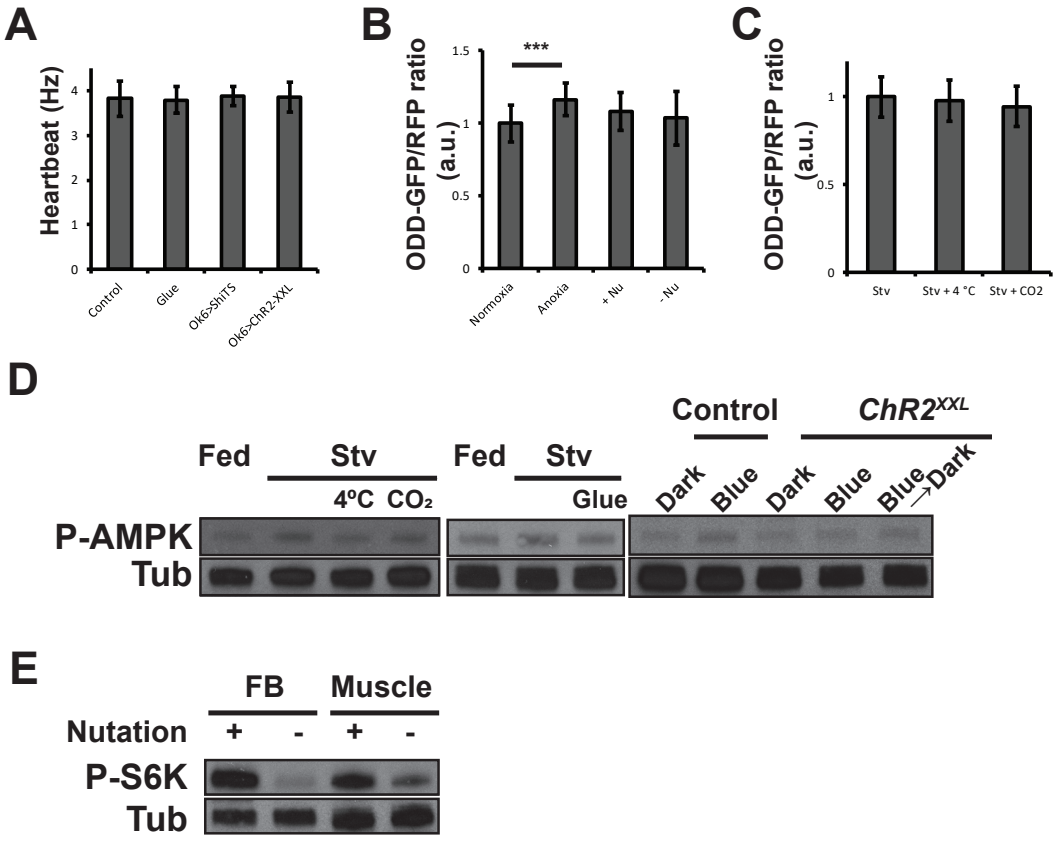

Supplemental Figure S2

(A) Measurement of heartbeat (Hz) of crawling larvae (Control, n=18) or larvae immobilized by glue (n=10), temperature shift-induced motor neuron inhibition (*Ok6>Shi^{TS}*, n=18) or blue light-induced motor neuron inhibition (*Ok6>ChR2^{XXL}*, n=4).

(B) Normalized ratio between Ubi::ODD-GFP and Ubi::RFP as shown in Fig. 2C-F. Normoxia in vivo n=13, anoxia in vivo n=17, ex vivo incubation with nutation n=13, and ex vivo without nutation n=16. ***p<0.001, student t-test.

(C) Normalized ratio between Ubi::ODD-GFP and Ubi::RFP in larvae paralyzed *in vivo* by 4 °C treatment (n=12) or CO_2 gas (n=14) for 15 min. Control n=12.

(D) Western blot of P-AMPK of fat body extracts from immobilized larvae as shown in Fig 1.B, C and Supplementary Fig. 1D.

(E) Fb-TOR activity of isolated fat body or body wall muscle displayed similar requirement for nutation during *ex vivo* incubation.

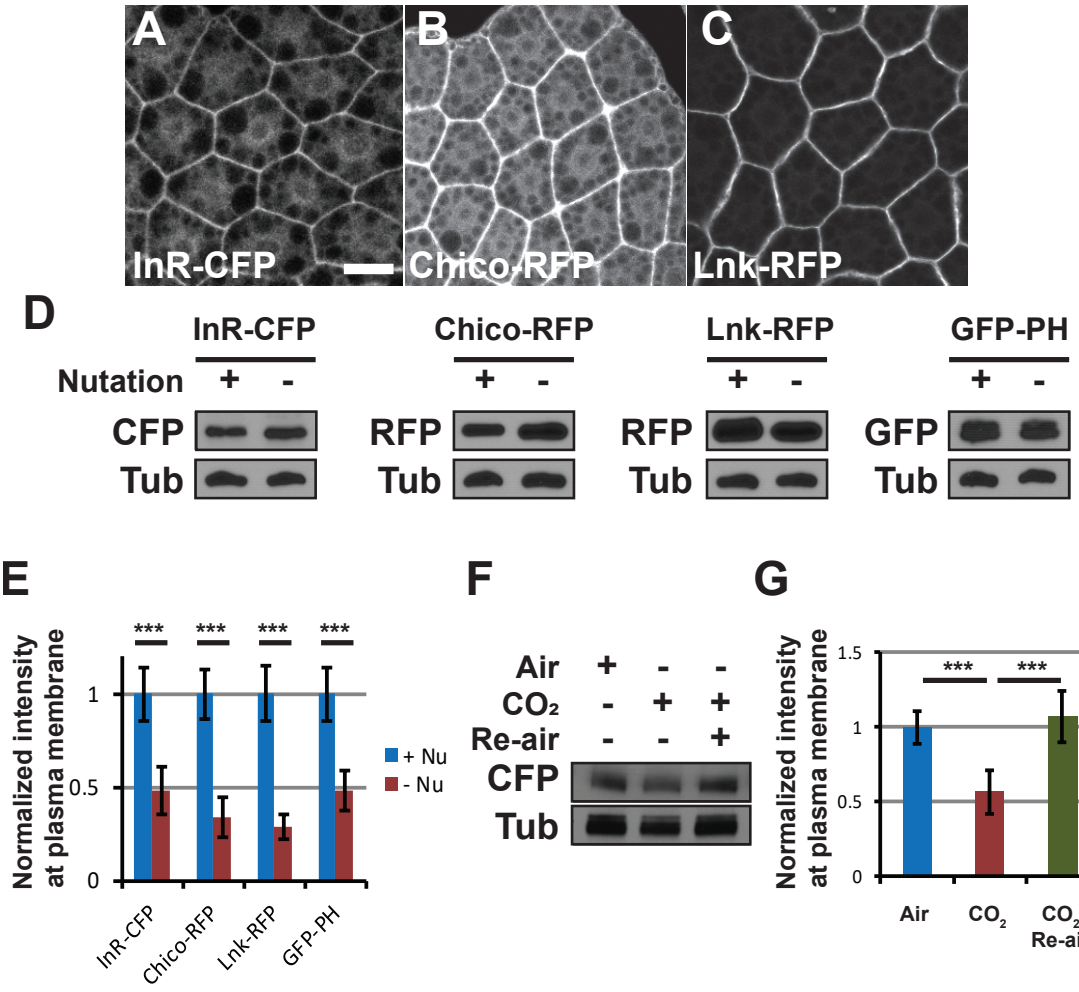

Supplemental Figure S3

(A-C) Localization of InR-CFP (A), Chico-RFP (B), or Lnk-RFP (C) in the fat body from larvae with normal crawling movement. Scale bar: 20 um.

(D) The protein levels of InR-CFP, Chico-RFP, Lnk-RFP and GFP-PH were measured by immunoblot after 2-hr *ex vivo* incubation in M3 + insulin media with or without mechanical stress.

(E) Normalized membrane signal intensity for the fluorescent markers shown in Figure 3A-H. A n=35, B n=40, C n=40, D n=50, E n=35, F n=30, G n=35, and H n=65. ***p<0.001, student t-test.

(F) Protein levels of InR-CFP under different body movement conditions shown in Figure 3I-K.

(G) Normalized membrane signal intensity of InR-CFP as shown in Figure 3I-K. I n=50, J n=40, and K n=45. ***p<0.001, student t-test.

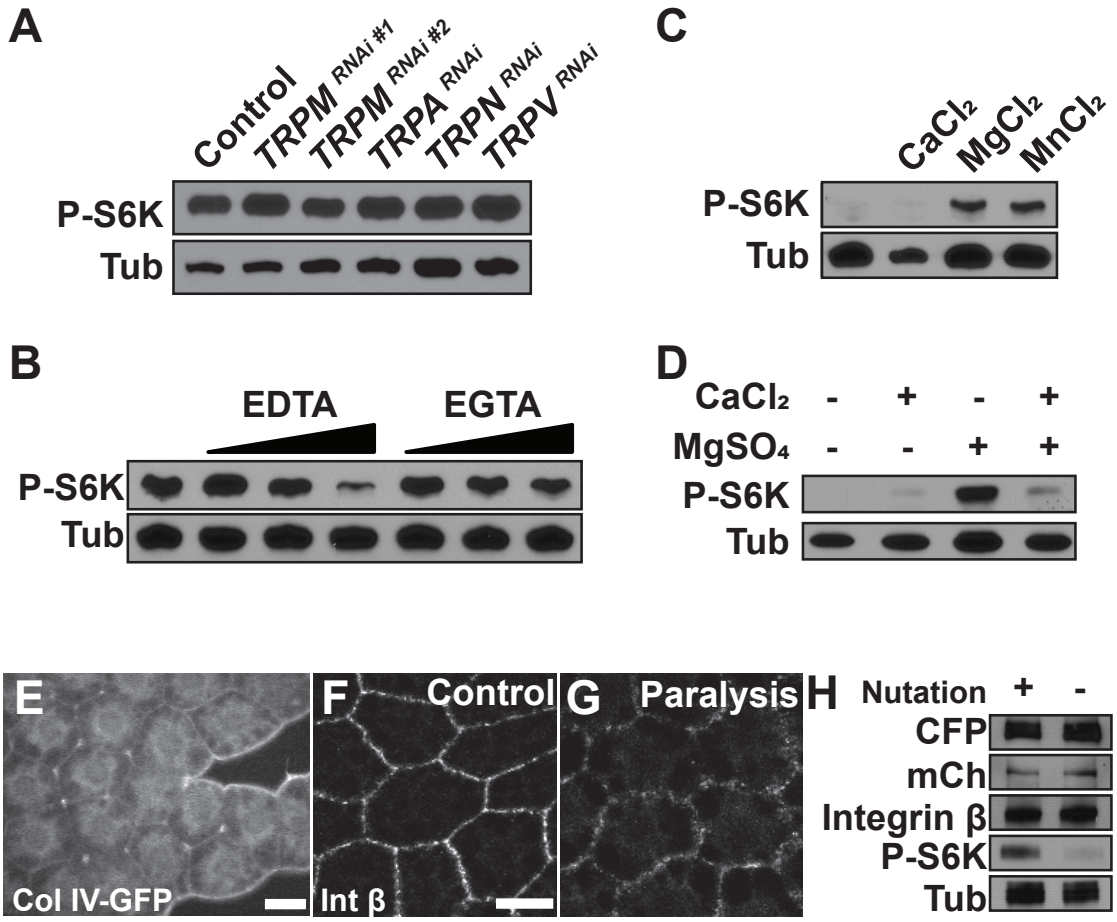

Supplemental Figure S4

(A) RNAi-mediated depletion of TRP channels (TRPM, TRPA, TRPN, or TRPV) did not affect fb-TOR in M3 media in the presence of insulin and nutation.

(B) Addition of EDTA (15, 30, and 60 mM) in the media inhibited fb-TOR dose-dependently with better efficiency compared to EGTA (15, 30, and 60 mM).

(C) Incubation in PBS containing 10 mM $MgCl_2$ or $MnCl_2$ but not $CaCl_2$ allowed activation of fb-TOR in the presence of insulin and nutation.

(D) $CaCl_2$ (10mM) antagonized $MgSO_4$ (10mM)-dependent activation of fb-TOR in PBS + insulin.

(E) Localization of Collagen IV (Vkg)-GFP around the periphery of larval fat body cells. Scale bar: 20 um.

(F, G) Integrin β staining in fat body from moving larvae (*Ok6-GAL4*, incubated at 37 °C for 30 min) (F) or larvae immobilized by motor neuron inhibition (*Ok6-GAL4 UAS-Shi^{TS}*, incubated at 37 °C for 30 min) (G). Scale bar: 20 um.

(H) Fat body protein levels of InR-CFP, Integrin β, and Talin-mCh are unaffected by nutation.

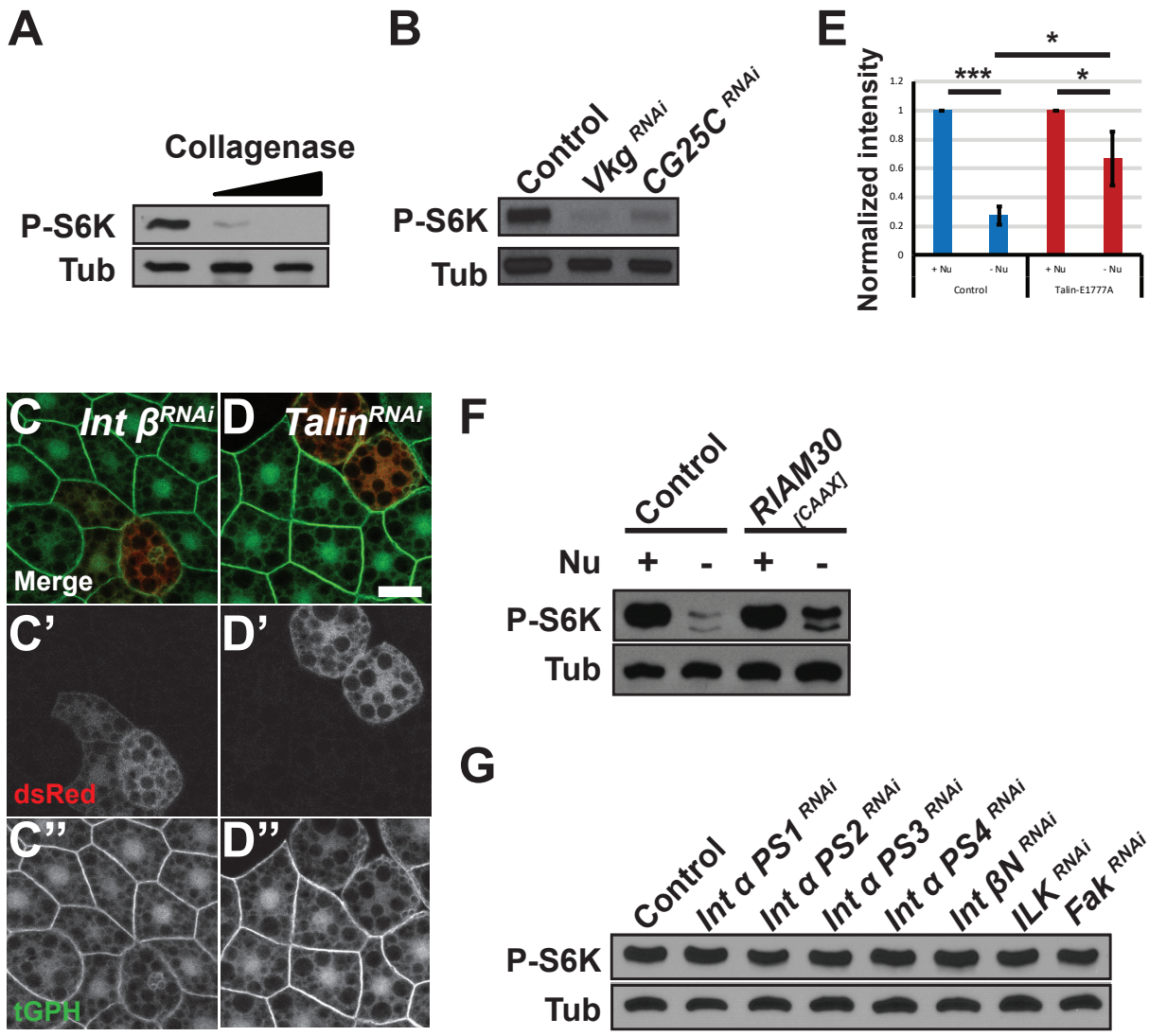

Supplemental Figure S5

(A) Addition of collagenase (10 and 50 ug/mL) in the M3 + insulin media *ex vivo* abolished mechanical stress-dependent fb-TOR activity.

(B) Depletion of collagen IV alpha 1 (CG25C) or collagen IV alpha 2 (Vkg) using hs-Gal4 decreased fb-TOR activity.

(C-D) Additional representative images contributing to the data shown in Figs. 5D and 5E.

(E) Quantification of four independent western blots as shown in Fig. 5F. * P<0.05, ***p<0.001, student t-test.

(F) *Ex vivo* fb-TOR activity was partially maintained in the absence of nutation in fat body expressing the integrin activator RIAM30-CAAX.

(G) RNAi-mediated depletion of integrin alpha PS1-4 *(mew, if, scb,* and *ItgaPS4)*, *integrin beta-N (βv), Ilk,* or *Fak* did not affect fb-TOR activity in the presence of insulin and nutation.

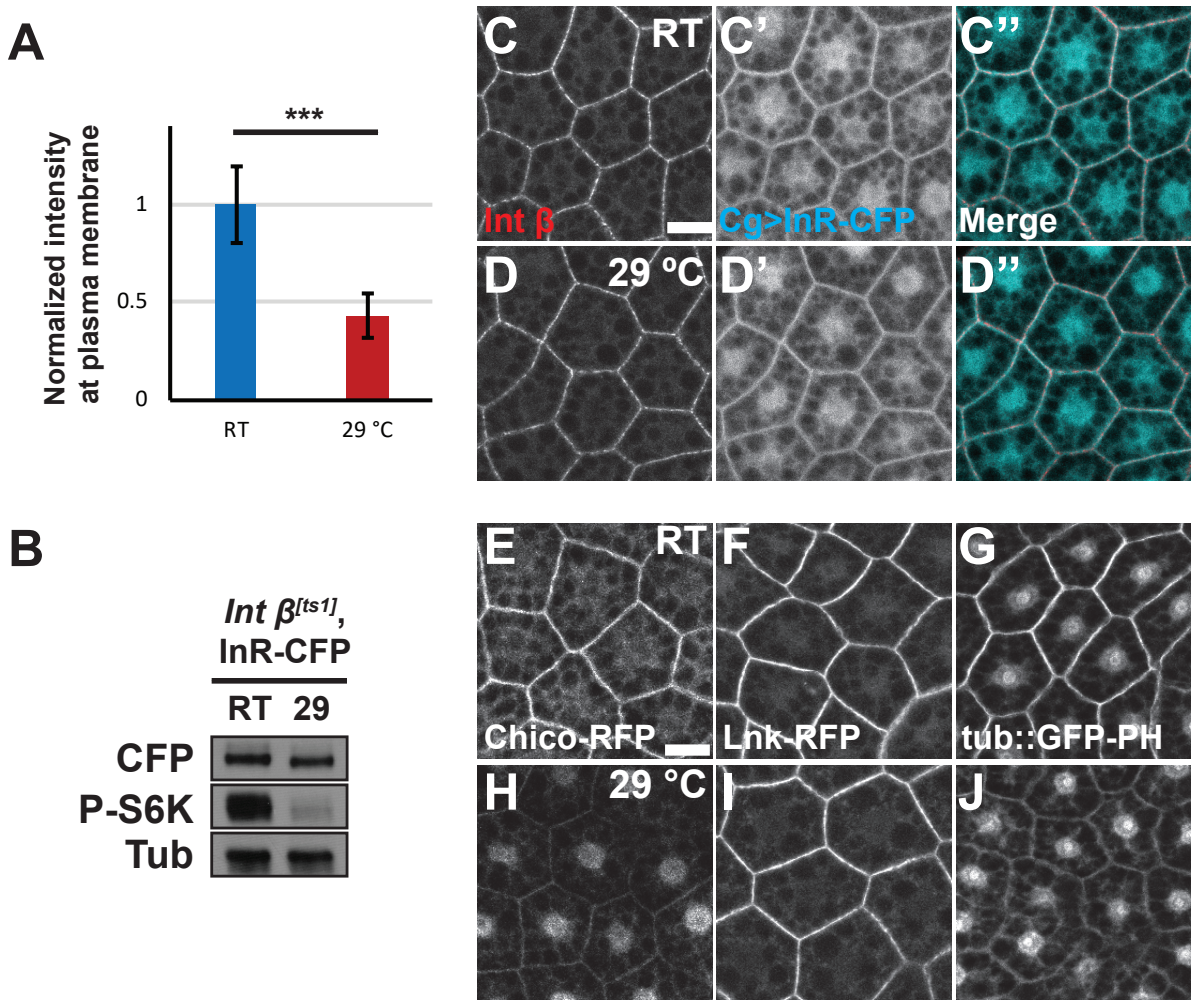

Supplemental Figure S6

(A) Normalized membrane signal intensity of InR-CFP in response to 29 °C inactivation of *Integrin β (mys^{ts1})*, as shown in Figure 5G (n=55) and 5H (n=55). ***p<0.001, student t-test.

(B) The protein level of InR-CFP in the fat body of *mys^{ts1}, Cg>InR-CFP* flies was not changed by temperature shift.

(C-D) Integrin β and InR-CFP remain localized to the cell membrane in the fat body of control *Cg>InR-CFP* flies after *ex vivo* incubation at permissive (C) or restrictive temperatures (D) in the presence of insulin and nutation. Scale bar: 20 um.

(E-J) Membrane localization of Chico-RFP, Lnk-RFP, and GFP-PH in the *mys^{ts1}* background at RT (E-G) or 29 °C (H-J). Scale bar: 20 um.

Supplemental Movie S1. Video of 3rd instar larva at room temperature. Crawling motion results in extensive undulating movement of the larval fat body, which is highlighted using Cg-GAL4 UAS-GFP.

Supplemental Movie S2. Video of 3rd instar larva after 15 minutes at 4 °C. Note the abolishment of crawling motion, and continued beating of the larval heart. Larval fat body is highlighted using Cg-GAL4 UAS-GFP.

Supplementary Table 1. *Drosophila melanogaster* strains used in this study

Drosophila line	**Reference**	**Source**
Act5c>CD2>GAL4[S]	[1]	Bloomington Drosophila Stock Center (BDSC)
Cg-GAL4.A2	[2]	BDSC
Hsp70-GAL4 [2-1]	[3]	BDSC
OK6-GAL4	[4]	BDSC
UAS-chico-RFP	[5]	gift of H. Stocker
UAS-Lnk-RFP	[5]	gift of H. Stocker
UAS-InR-CFP	[5]	gift of H. Stocker
Ubi-Talin^{E1777A}-GFP	[6]	gift of G. Tanentzapf
UAS-mCh-RIAM30-RAP1[CAAX]	[6]	gift of G. Tanentzapf
UAS-WT-Dp110	[7]	BDSC
UAS-Rheb [EP50.084]	[8]	gift of E. Hafen
UAS-shi^{ts1}K3	[9]	BDSC
UAS-ChR2-XXL	[10]	BDSC
	[11]	
Ubi::ODD-GFP		Gift of S. Luschnig
mys$^{[ts1]}$	[12]	BDSC
tGPH[2]	[13]	BDSC
Vkg::GFP [G00205]	[14]	Gift of L. Cooley
Talin (rhea)-mCherry [MI00296]	[15]	BDSC
UAS-Talin (rhea) RNAi [TRiP.HMS00856]	[16]	BDSC
UAS-Integrin beta (mys) RNAi [TRiP.HMS00043]	[16]	BDSC
UAS-Integrin alpha PS1 (mew) RNAi [TRiP.HMS02849]	[16]	BDSC
UAS-Integrin alpha PS2 (if) RNAi [TRiP.JF02695]	[16]	BDSC
UAS-Integrin alpha PS3 (scb) RNAi [TRiP.HMS01873]	[16]	BDSC
UAS-ItgaPS4 RNAi [TRiP.HMC02928]	[16]	BDSC
UAS-Itgbn RNAi [TRiP.HM05089]	[17]	BDSC
UAS-Ilk RNAi [TRiP.HMS04509]	[16]	BDSC
UAS-Fak RNAi [TRiP.HMS00010]	[16]	BDSC
UAS-TRPM RNAi #1 [TRiP.HMC03236]	[16]	BDSC
UAS-TRPM RNAi #2 [TRiP.JF01236]	[17]	BDSC
UAS-TRPA (pain) RNAi [TRiP.JF01065]	[17]	BDSC
UAS-TRPN (nompC) RNAi [TRiP.JF01067]	[17]	BDSC
UAS-TRPV (iav) RNAi [TRiP.JF01904]	[17]	BDSC
UAS-vkg RNAi {KK111668}VIE-260B	[18]	Vienna Drosophila RNAi Center
UAS-Col4a1 RNAi [TRiP. HMC02910]	[19]	BDSC

References

1. Pignoni, F. and S.L. Zipursky, *Induction of Drosophila eye development by decapentaplegic.* Development, 1997. **124**(2): p. 271-8.

2. Hennig, K.M., J. Colombani, and T.P. Neufeld, *TOR coordinates bulk and targeted endocytosis in the Drosophila melanogaster fat body to regulate cell growth.* J Cell Biol, 2006. **173**(6): p. 963-74.
3. Brand, A.H. and N. Perrimon, *Targeted gene expression as a means of altering cell fates and generating dominant phenotypes.* Development, 1993. **118**(2): p. 401-15.
4. Sanyal, S., *Genomic mapping and expression patterns of C380, OK6 and D42 enhancer trap lines in the larval nervous system of Drosophila.* Gene Expr Patterns, 2009. **9**(5): p. 371-80.
5. Almudi, I., et al., *The Lnk/SH2B adaptor provides a fail-safe mechanism to establish the Insulin receptor-Chico interaction.* Cell Commun Signal, 2013. **11**(1): p. 26.
6. Ellis, S.J., et al., *Talin autoinhibition is required for morphogenesis.* Curr Biol, 2013. **23**(18): p. 1825-33.
7. Weinkove, D., et al., *Regulation of imaginal disc cell size, cell number and organ size by Drosophila class I(A) phosphoinositide 3-kinase and its adaptor.* Curr Biol, 1999. **9**(18): p. 1019-29.
8. Stocker, H., et al., *Rheb is an essential regulator of S6K in controlling cell growth in Drosophila.* Nat Cell Biol, 2003. **5**(6): p. 559-66.
9. Kitamoto, T., *Conditional modification of behavior in Drosophila by targeted expression of a temperature-sensitive shibire allele in defined neurons.* J Neurobiol, 2001. **47**(2): p. 81-92.
10. Dawydow, A., et al., *Channelrhodopsin-2-XXL, a powerful optogenetic tool for low-light applications.* Proc Natl Acad Sci U S A, 2014. **111**(38): p. 13972-7.
11. Misra, T., et al., *A genetically encoded biosensor for visualising hypoxia responses in vivo.* Biol Open, 2017. **6**(2): p. 296-304.
12. Deak, II, et al., *Mutations affecting the indirect flight muscles of Drosophila melanogaster.* J Embryol Exp Morphol, 1982. **69**: p. 61-81.
13. Britton, J.S., et al., *Drosophila's insulin/PI3-kinase pathway coordinates cellular metabolism with nutritional conditions.* Dev Cell, 2002. **2**(2): p. 239-49.
14. Morin, X., et al., *A protein trap strategy to detect GFP-tagged proteins expressed from their endogenous loci in Drosophila.* Proc Natl Acad Sci U S A, 2001. **98**(26): p. 15050-5.
15. Venken, K.J., et al., *MiMIC: a highly versatile transposon insertion resource for engineering Drosophila melanogaster genes.* Nat Methods, 2011. **8**(9): p. 737-43.
16. Ni, J.Q., et al., *A genome-scale shRNA resource for transgenic RNAi in Drosophila.* Nat Methods, 2011. **8**(5): p. 405-7.
17. Ni, J.Q., et al., *A Drosophila resource of transgenic RNAi lines for neurogenetics.* Genetics, 2009. **182**(4): p. 1089-100.
18. Dietzl, G., et al., *A genome-wide transgenic RNAi library for conditional gene inactivation in Drosophila.* Nature, 2007. **448**(7150): p. 151-6.
19. Crest, J., et al., *Organ sculpting by patterned extracellular matrix stiffness.* Elife, 2017. **6**.